Equilibration Processes in Sphaleron Transitions

D.Yu.Grigoriev

Institute for Nuclear Research of Russian Academy of Sciences,

117312 Moscow, Russia

Abstract

Sphaleron transitions in the course of thermalization of highly non-equilibrium initial field configurations are numerically investigated in (1+1)-dimensional Abelian two-Higgs model. It is shown that the transition rate is sensitive to deviations from thermal equilibrium. The process of thermalization can be very slow and is getting even more slower for configurations with low total energies.

In recent years, an equilibrium rate of thermal sphaleron transitions has been thoroughly studied in wide temperature range both analytically and numerically [1-17]. However, many modern scenarios for baryogenesis are based on rather complicated dynamical phenomena (e.g. propagating domain walls) that by its nature are strongly non-equilibrium. Better understanding of when we really can use equilibrium approaches is also required in the study of parametric resonance and its applications to cosmology, where at the end of resonance at least some of the fields involved are left in highly excited states [18-20].

Here we numerically investigate the process of thermalization for two non-equilibrium initial configurations. While the energy of the first configuration is localised in low-momentum modes, the second one represents relatively high-momentum state (in respect to the spatial scale of sphaleron). It is shown that the thermalization process can take a considerable amount of time; this amount strongly depends on the total energy of the system, or, in other words, the equilibrium temperature finally reached. The sphaleron transition rate is very sensitive to deviations of the system from equilibrium, although the rate approaches its equilibrium value generally on the same time scale as the field spectra take their normal thermal shape. More detailed quantitative study of the transition rate variations and its relation to evolution of the spectra will be discussed in a separate paper [21].

The simulations presented below were carried out in the same (1+1)-dimensional two-Higgs Abelian model used in ref. [22]:

$$\mathcal{L} = -\frac{1}{4}{F_{\mu\nu}}^2 + (D_\mu\phi_1)^\dagger(D_\mu\phi_1) + (D_\mu\phi_2)^\dagger(D_\mu\phi_2) - V(\phi_1,\phi_2)$$

$$\begin{aligned} V(\phi_1,\phi_2) &= \lambda_1(\phi_1^\dagger\phi_1 - {v_1}^2)^2 + \lambda_2(\phi_2^\dagger\phi_2 - {v_2}^2)^2 + \\ &\quad \lambda_3(\phi_1^\dagger\phi_1 + \phi_2^\dagger\phi_2 - {v_1}^2 - {v_2}^2)^2 + \\ &\quad \lambda_5(Re(\phi_1^\dagger\phi_2) - v_1 v_2\cos\xi_0)^2 + \lambda_6(Im(\phi_1^\dagger\phi_2) - v_1 v_2 \sin\xi_0)^2 \end{aligned}$$

where $\lambda_1 = \lambda_2 = \lambda_3 = 1$, $\lambda_5 = \lambda_6 = 0.5$, $v_1 = v_2 = 1$, $\xi_0 = 0$.

In fact, the second Higgs field has no serious effect on equilibration dynamics; however, it's presence is useful for filtering out the thermal noise in the process of counting the sphaleron transitions, because real transitions correspond to simultaneous changes in winding numbers of both scalar fields coupled with the gauge field A. The first configuration is studied on the lattice with $N = 500$ sites and the size of $L = 50$, while for the second configuration the size was reduced to $L = 10$.

The temperature dependence of equilibrium transition rate Γ for both $L = 50$ and $L = 10$ is presented on Figs. 1 and 2. Note that direct sphaleron counting technique used throughout this study prevents us from getting reliable data for high-T region where the dependence $\Gamma(T)$ can no longer be approximated by simple Boltzmann exponent.

Initially almost all energy of the first configuration is localised at the Higgs field $\phi_1 \sim \sin(\pi x/L)$ (one half-wave). The number of sphaleron transitions accumulated in the course of real-time evolution is presented on Fig. 3 as a function of time t. The transition to equilibrium regime (solid line on Fig. 3) occurs at t about $10...20 \cdot 10^3$. The evolution of spectrum of scalar fields is presented on Figs. 4-7.

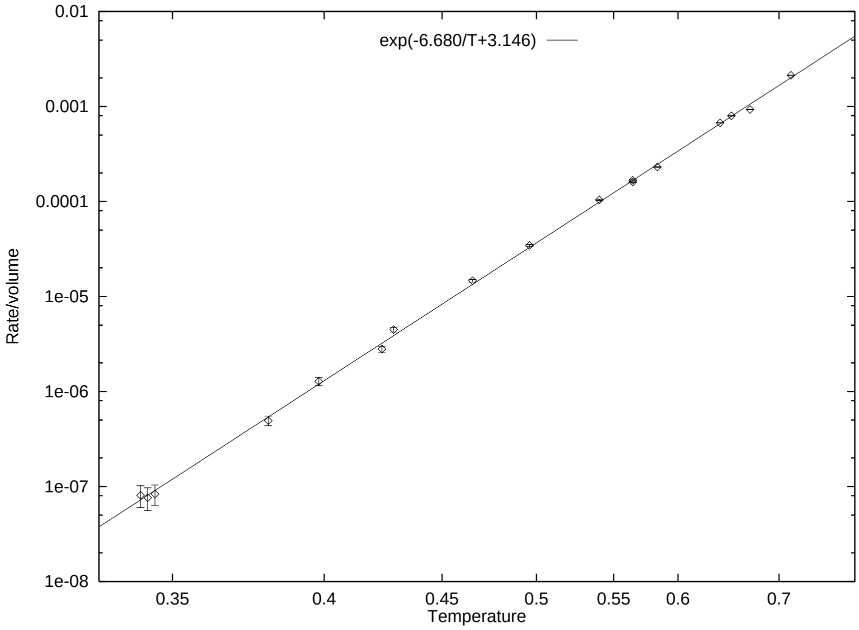

Figure 1: Sphaleron transition rate Γ as a function of dimensionless temperature T for lattice volumes $L = 25$ and $L = 50$ (combined). Solid line is the best exponential approximation to data. The first run presented below on Figs. 3-7 has the (conserving) energy $E = 749$ which corresponds to $T = 0.3745$, $\Gamma = 4.17 \cdot 10^{-7}$ and expected time between transitions $\tau = (L \cdot \Gamma)^{-1} = 48000$.

In the second configuration the scalar field ϕ_1 is close to $sin(50 \cdot 2\pi x/L)$, while the characteristic spatial momentum of the sphaleron for actual parameters of Higgs potential ($v_1 = v_2$ etc.) can be estimated as $k_{sph} \sim v \cdot \sqrt{\lambda_1 + \lambda_2 + 4\lambda_3 + \lambda_5} \sim 2.5 \sim 4 \cdot 2\pi/L$. Because both the spatial volume of this configuration and its energy (controlled by the initial amplitude of ϕ_1) are lower than in the first run (Figs. 3-7), the equilibrium transition rate decreases correspondingly, and the time interval τ between two subsequent transitions is expected to be of order $\tau \sim 810000$. These purely thermal transitions are too rare to be observed using available computing resources, so the major goal of the second example is to show that a slight (6%) decrease in energy (i.e. temperature) may greatly increase the thermalization time. Fig. 8 presents the dynamics of sphaleron transitions for

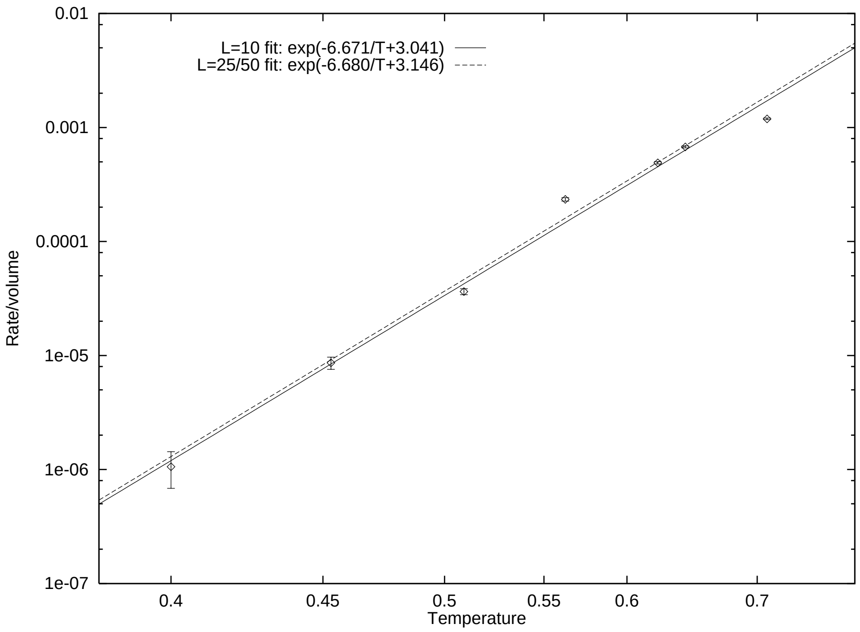

Figure 2: $\Gamma(T)$ for $L = 10$. The exponential fit (solid line) is compared to that one from Fig.1. The second run (Figs. 8-18) has $E = 704$ corresponding to $T = 0.352$ and $\tau = 810000$.

the second configuration; it's important to note that because the equilibrium transition rate is virtually negligible (less than one transition per the whole plot of Fig. 8), all the transitions present on Fig. 8 are of non-equilibrium nature. The evolution of field spectra is presented on Figs. 9-18; note that their equilibration is also considerably slower than that one on Figs. 4-7.

Finally, it's interesting to notice how differently the sphaleron transitions occur on early stages of evolution in both configurations (Figs. 19 and 20): for short-wave initial configuration, the transitions are suppressed at the beginning of evolution. A probable reason is slow propagation of energy to sphaleron-related spectral modes in this case.

The author is indebted to J.Baacke, L.McLerran, V.Rubakov, A.Smilga, M.Shaposhnikov and M.Tsypin for stimulating questions and discussions. This study was supported by RBRF grant 96-02-17804a.

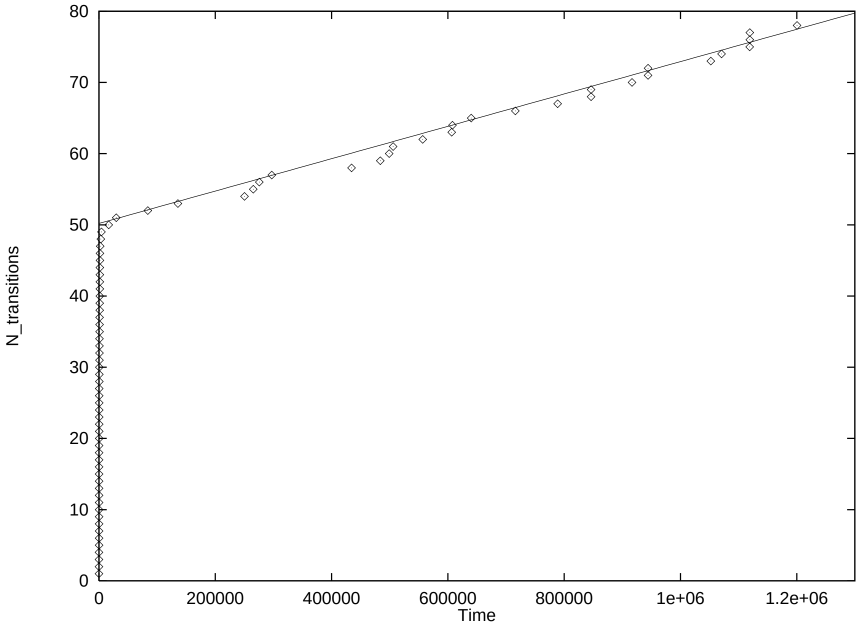

Figure 3: Sphaleron transition dynamics for the first run (see also Fig. 19). Solid line corresponds to time interval between transitions $\tau = 44000$.

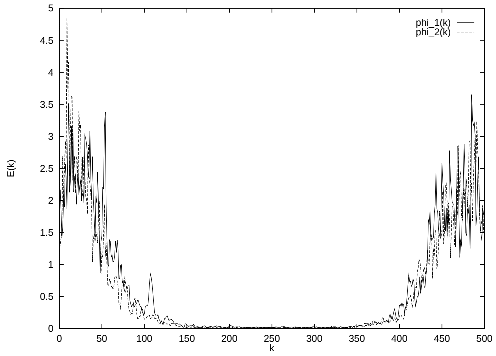

Figure 4: Energy spectrum $E(k)$ of scalar fields ϕ_1 and ϕ_2 at time $t = 40$ (initial spectrum not shown). Mode number N (axis x) is related to physical momentum k as $k = \frac{2\pi}{L}N$. Note that because of periodicity in N the right-hand part of the plot corresponds to low-momentum modes with negative k.

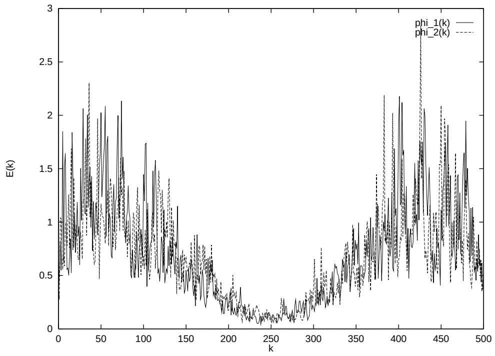

Figure 5: Energy spectrum at $t = 1080$

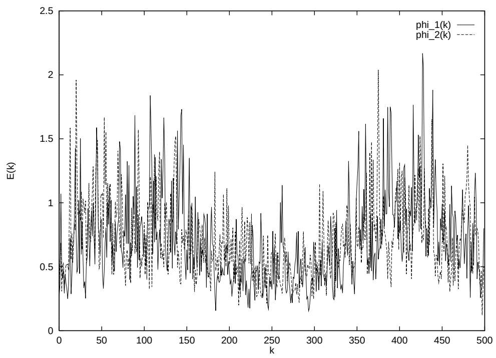

Figure 6: Energy spectrum at $t = 5000$

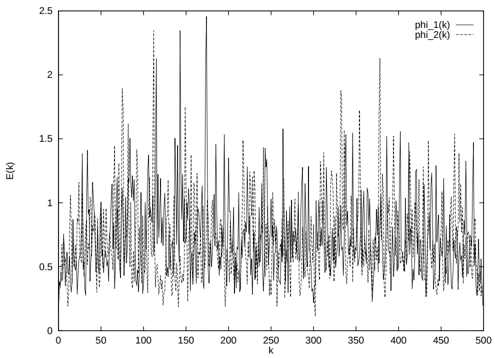

Figure 7: Energy spectrum at $t = 15000$

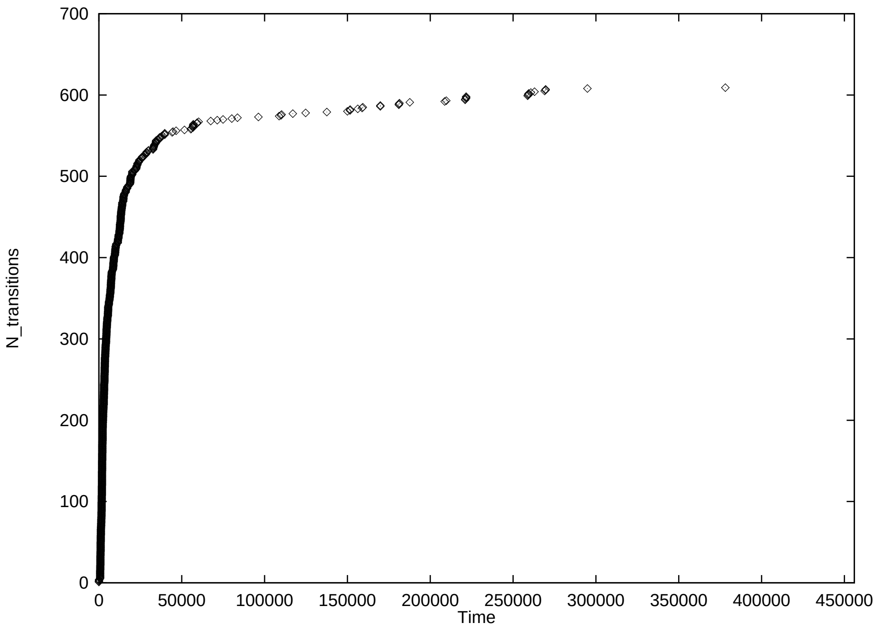

Figure 8: Sphaleron transition dynamics for the second run (see also Fig. 20). Estimated thermal rate corresponds to average time between transitions $\tau \sim 810000$.

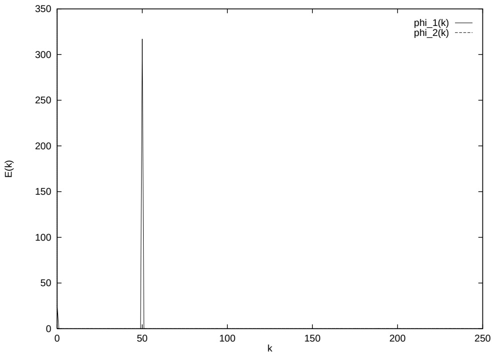

Figure 9: Energy spectrum $E(k) + E(-k)$ of scalar fields ϕ_1 and ϕ_2 at $t = 0$ (initial state). Mode number N (axis x) is related to physical momentum k as $k = \frac{2\pi}{L}N$.

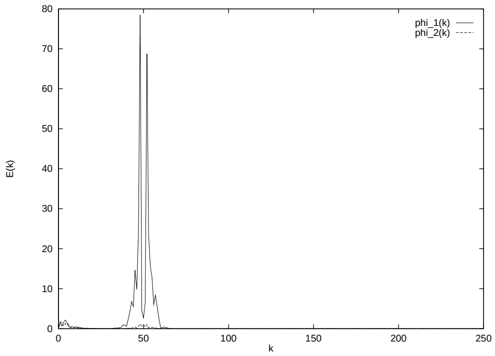

Figure 10: Energy spectrum at $t = 40$

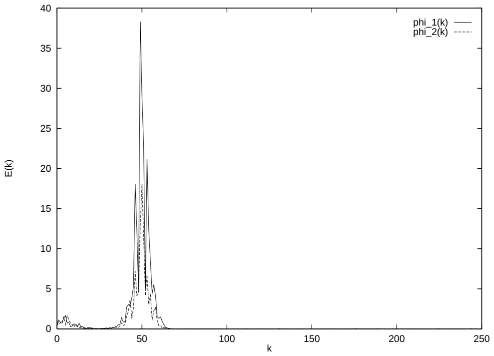

Figure 11: Energy spectrum at $t = 72$

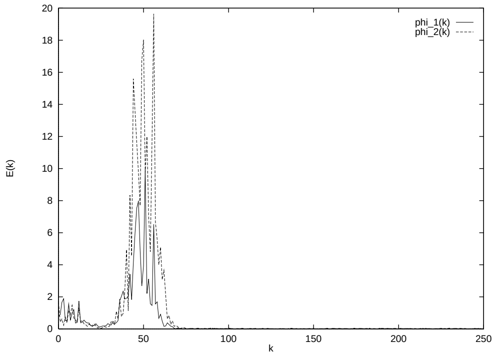

Figure 12: Energy spectrum at $t = 160$

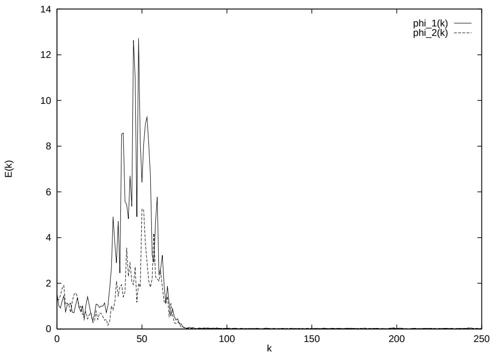

Figure 13: Energy spectrum at $t = 240$

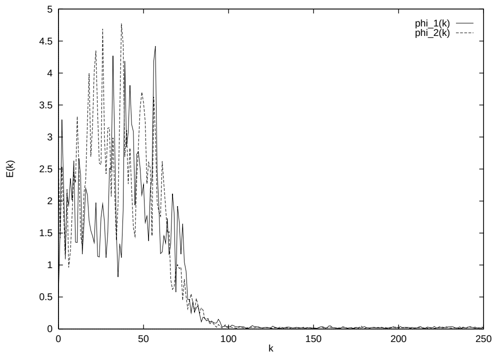

Figure 14: Energy spectrum at $t = 480$

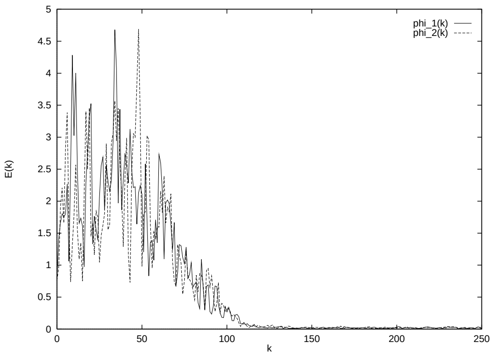

Figure 15: Energy spectrum at $t = 1000$

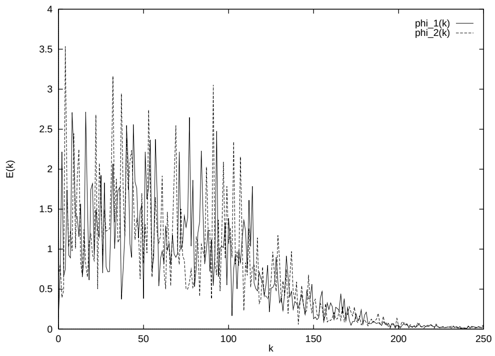

Figure 16: Energy spectrum at $t = 11000$

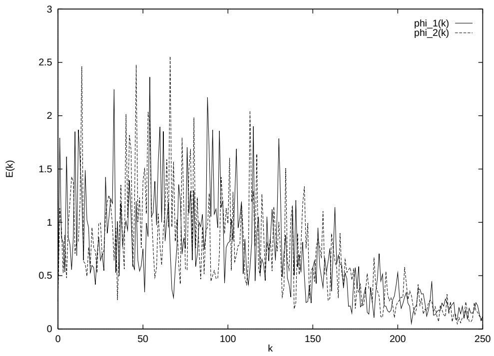

Figure 17: Energy spectrum at $t = 70000$

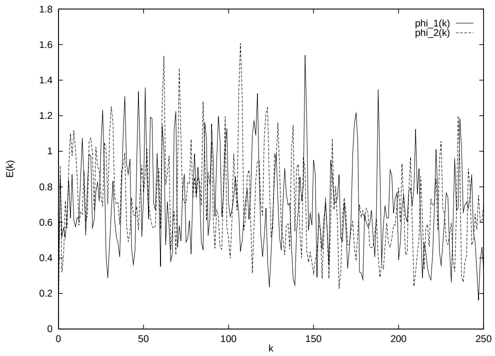

Figure 18: Energy spectrum at $t = 456000$

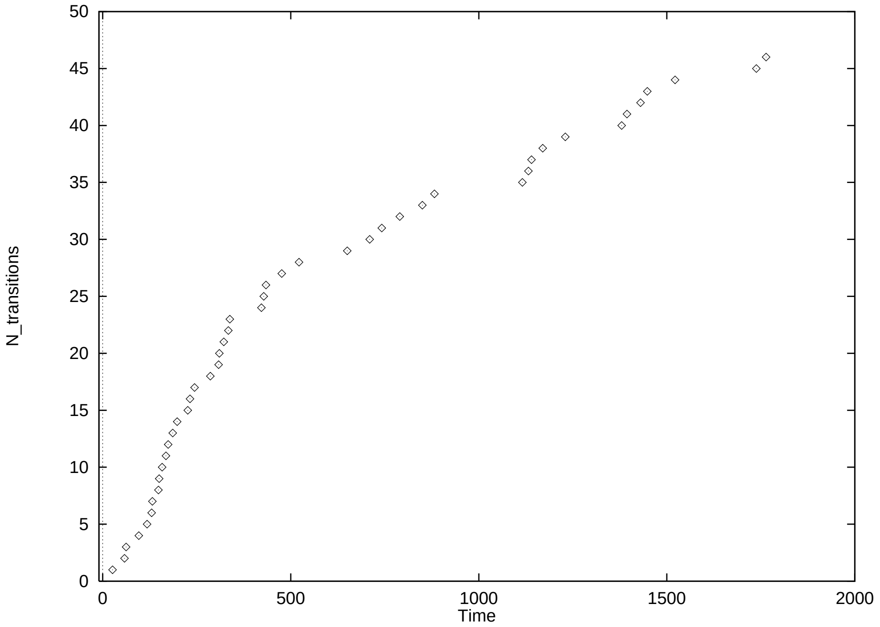

Figure 19: Initial part of plot Fig. 3.

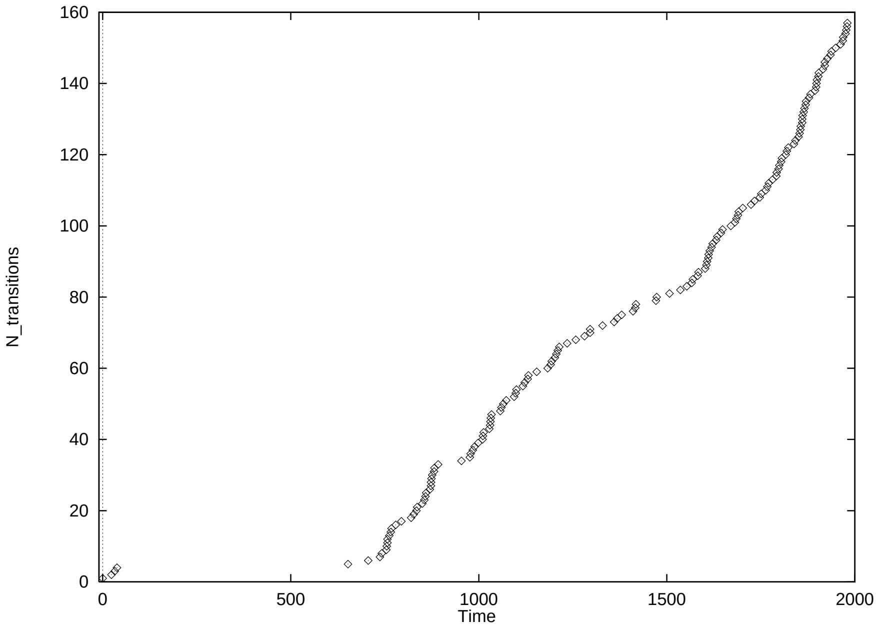

Figure 20: Initial part of plot Fig. 8.

References

[1] P.Arnold and L.McLerran, Phys.Rev.D36(1987)581

[2] A.I.Bochkarev and G.G.Tsitsishvili, Phys.Rev.D40(1989)1378.

[3] D.Yu.Grigoriev and V.A.Rubakov, Nucl.Phys.B299(1988)67.

[4] D.Yu.Grigoriev, V.A.Rubakov and M.E.Shaposhnikov, Phys.Lett.B216 (1989)172; Nucl.Phys.B326(1989)737.

[5] J.Ambjørn, T.Askgaard, H.Porter and M.E.Shaposhnikov, Phys.Lett. B244(1990)479; Nucl.Phys.B353(1991)346

[6] A.I.Bochkarev and Ph. de Forcrand, Phys.Rev.D44(1991)519

[7] D.Bödeker, L.McLerran and A.Smilga, Phys.Rev.D52(1995)4675.

[8] Ph. de Forcrand, A.Krasnitz and R.Potting, Phys.Rev.D50(1994)6054.

[9] J.Ambjørn and A.Krasnitz, Phys.Lett.B362(1995)97; Nucl.Phys.B506 (1997)387.

[10] J.Smit and W.H.Tang, Nucl.Phys. B (Proc.Suppl.) 42(1995)590.

[11] W.H.Tang and J.Smit, Nucl. Phys. B482(1996)265.

[12] W.H.Tang and J.Smit, preprint ITFA-98-08, hep-lat/9805001.

[13] G.D.Moore and N.G.Turok, Phys.Rev.D56(1997)6533.

[14] G.D.Moore, C.H.Hu and B.Müller, Phys.Rev.D58(1998)045001.

[15] P.Arnold, D.T.Son and L.G.Yaffe, Phys.Rev.D55(1997)6264.

[16] P.Arnold, Phys.Rev.D55(1997)7781.

[17] L.G.Yaffe, talk at International Seminar "Quarks-98", Suzdal, 1998.

[18] S.Yu.Khlebnikov and I.I.Tkachev, Phys.Rev.Lett.77(1996)219.

[19] S.Yu.Khlebnikov and I.I.Tkachev, Phys.Rev.Lett.79(1997)1607.

[20] T.Prokopec and T.G.Roos, Phys.Rev.D55(1997)3768.

[21] D.Yu.Grigoriev, in preparation.

[22] D.Yu.Grigoriev, M.E.Shaposhnikov and N.G.Turok, Phys.Lett.B275 (1992)395.